

*Reprinted from*

JAPANESE JOURNAL OF  
**APPLIED  
PHYSICS**

**REGULAR PAPER**

**Conversion Efficiency of Intermediate Band Solar Cells with GaAs:N  $\delta$ -Doped Superlattices**

Shuhei Yagi, Shunsuke Noguchi, Yasuto Hijikata, Shigeyuki Kuboya, Kentaro Onabe, and Hiroyuki Yaguchi

Jpn. J. Appl. Phys. **52** (2013) 102302

## Conversion Efficiency of Intermediate Band Solar Cells with GaAs:N $\delta$ -Doped Superlattices

Shuhe Yagi<sup>1\*</sup>, Shunsuke Noguchi<sup>1</sup>, Yasuto Hijikata<sup>1</sup>, Shigeyuki Kuboya<sup>2</sup>, Kentaro Onabe<sup>3</sup>, and Hiroyuki Yaguchi<sup>1</sup>

<sup>1</sup>Graduate School of Science and Engineering, Saitama University, Saitama 338-8570, Japan

<sup>2</sup>Institute for Materials Research, Tohoku University, Sendai 980-8577, Japan

<sup>3</sup>Department of Advanced Materials Science, The University of Tokyo, Kashiwa, Chiba 277-8583, Japan

E-mail: yagi@opt.ees.saitama-u.ac.jp

Received June 15, 2013; revised July 29, 2013; accepted July 30, 2013; published online October 1, 2013

The performance of intermediate band solar cells using a GaAs:N  $\delta$ -doped superlattice (SL) as the optical absorber is analyzed. In GaAs:N  $\delta$ -doped SLs, both of the  $E_+$  and  $E_-$  bands formed around the N  $\delta$ -doped layers form SL potentials with the conduction band of the spacer GaAs layers, resulting in the formation of multiple minibands. The conversion efficiency limits of the solar cells are calculated using the detailed balance model based on intermediate band structures composed of the valence band and two minibands formed respectively in the  $E_-$ - and  $E_+$ -related SL potentials. A high efficiency of 62.6% for full concentration is expected by properly adjusting the structural parameters of the SL. Alloying other elements such as In to a GaAs:N  $\delta$ -doped SL is a possible way to further facilitate the development of intermediate band materials for high-efficiency solar cells. © 2013 The Japan Society of Applied Physics

### 1. Introduction

Dilute nitride alloys such as GaAsN have attracted attention as an intermediate band material for high-efficiency intermediate band solar cells (IBSCs).<sup>1–3)</sup> N addition into GaAs modifies the electronic structure, and the conduction band (CB) edge energy of GaAsN is reduced with increasing N content. In addition, a new energy band usually labeled the  $E_+$  band is formed above the original CB (labeled  $E_-$  band). These  $E_+$  and  $E_-$  bands and the valence band (VB) are considered to constitute an intermediate band energy structure, which has been proven by means of modulation spectroscopy by many researchers.<sup>4–7)</sup> Although IBSCs with a GaAsN absorber were demonstrated,<sup>2,3)</sup> improvement in the solar cell performance as expected has not been achieved yet. The high immiscibility of nitrogen into GaAs disturbs uniform nitrogen incorporation into the substitutional sites. This results in the potential fluctuation at the CB edge<sup>8–10)</sup> and the short diffusion length of photogenerated carriers.

Recently, Ishikawa et al. have shown the possibility of direct bandgap engineering in GaAs by a N  $\delta$ -doping technique.<sup>11)</sup> They demonstrated a redshift of the fundamental bandgap of GaAs in which N  $\delta$ -doped layers were inserted. The  $\delta$ -doping technique enables us to incorporate atoms with mismatched covalent radii into substitutional sites in a host material matrix, without destruction of the crystal perfection.<sup>12)</sup> More recently, we have found that the electronic structure in an energy range higher than the GaAs bandgap is modified as well by periodic insertion of N  $\delta$ -doped layers into GaAs.<sup>13,14)</sup> In these GaAs:N  $\delta$ -doped superlattices (SLs), a number of new energy bands are formed both at the lower and higher energy sides of the GaAs bandgap. The intensity of photoreflectance (PR) signals from optical transitions associated with the higher energy bands are strongly enhanced compared with the  $E_+$  band transitions in uniformly N-doped GaAsN alloys. Because of their superior transition properties, we have proposed GaAs:N  $\delta$ -doped SLs as an alternative material for the absorber of IBSCs. In this paper, the potential of this material system for IBSCs is discussed on the basis of the estimation of the solar cell characteristics by means of the detailed balance calculation.

### 2. Experimental Methods

Samples were grown by metalorganic vapor phase epitaxy (MOVPE) using trimethylgallium (TMG), tertiarybutylarsine (TBAs) and dimethylhydrazine (DMHy) as the Ga, As, and N sources, respectively. A GaAs buffer layer was grown on a GaAs(001) substrate followed by the growth of a 30 period SL of GaAs/N  $\delta$ -doped layers. N  $\delta$ -doped layers were formed by supplying DMHy while GaAs growth is stopped. The SL was fabricated by repeating the formation of the  $\delta$ -doped layer and GaAs spacer layer. A 20-nm-thick GaAs cap layer was grown on top of the SL. The fine structure of periodic N  $\delta$ -doped layers was confirmed by secondary ion mass spectroscopy (SIMS), the N profiles of which were quantified by comparison with ion-implanted standard samples. The average N content in the SL region, the N area density in a  $\delta$ -doped layer, and the SL period (almost identical to the spacer GaAs layer thickness) were determined by a SIMS profile, and were 0.15%,  $2.4 \times 10^{13} \text{ cm}^{-2}$ , and 6.9 nm, respectively. Uniformly N-doped GaAsN alloys were also prepared as references.

PR measurements were carried out to investigate the optical properties of the samples. In the PR measurements, a diode pumped solid-state (DPSS) laser at 532 nm was used as a modulation light. A probe light, which illuminates the sample surface in a cryostat, was obtained from a halogen lamp through a monochromator. PR signals were detected by a Si photodiode using a phase-sensitive lock-in amplification system.

### 3. Results and Discussion

Figure 1 shows PR spectra of the GaAs:N  $\delta$ -doped SL and uniformly N-doped GaAsN (N content: 0.11–0.74%) measured at 120 K. The arrows in the figure indicate the transition energies estimated by fitting with Aspnes's third-derivative functional form.<sup>15)</sup> The oscillatory features above the GaAs bandgap transitions observed in the spectra of GaAsN are the Franz–Keldysh oscillations (FKOs).<sup>16)</sup> For all the samples, a PR transition signal was observed below the GaAs bandgap energy, which originates from the  $E_-$  band in the N-containing layers. In addition, a number of strong transition signals, which have different features from the FKOs in the GaAsN spectra, are detected only for the SL in an energy

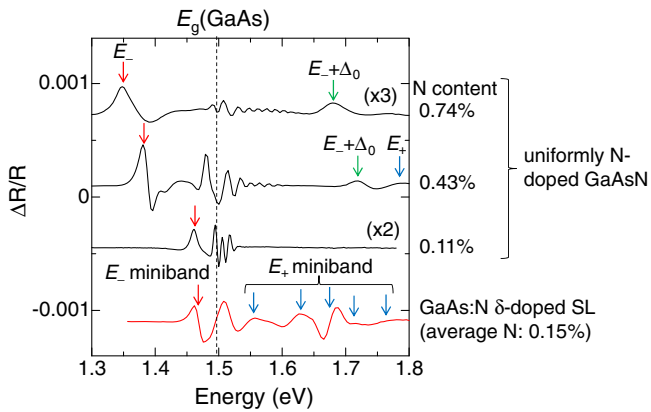


**Fig. 1.** (Color online) PR spectra of uniformly N-doped GaAs (N content: 0.11–0.74%) and a GaAs:N  $\delta$ -doped superlattice (average N content: 0.15%) measured at 120 K.

range from 1.55 to 1.78 eV. No transitions are observed in this energy range in uniformly N-doped GaAsN with a comparable N content. Because the spin–orbit split-off energy of GaAs(N) is 0.33 eV<sup>7)</sup> and the  $E_-$ -related transition of the SL is observed at 1.47 eV, the spin–orbit split-off to conduction band transitions do not explain the transitions below 1.8 eV. These characteristic energy positions of the optical transitions in the SL can be interpreted by considering the SL potentials composed of the GaAs CB and the modulated CBs around the N  $\delta$ -doped layers.<sup>13,14)</sup> The energy structure of a GaAs:N  $\delta$ -doped SL is schematically illustrated in Fig. 2. A N  $\delta$ -doped layer and its neighboring GaAs layers behave as a thin GaAsN layer with an effective width, and thus the  $E_+$  and  $E_-$  bands are formed around the N  $\delta$ -doped layers. These modulated CBs contribute to the formation of SL minibands. The  $E_+$  band around a  $\delta$ -doped layer and the GaAs CB work as a barrier and a well, respectively, and resulting minibands are formed between the  $E_+$  band edge and the GaAs CB edge [Fig. 2(c)]. Multiple electron transition pathways associated with the  $E_+$  minibands are expected and the energy range of these transitions between

the  $E_+$  miniband edges and VB is in good agreement with that of the PR signals observed at 1.55–1.78 eV. Therefore, the PR signals at the higher energy side of the GaAs bandgap energy are attributed to transitions associated with the minibands in the  $E_+$  band/GaAs CB SL potential while the lower PR signal at 1.47 eV is due to the miniband in the  $E_-$  band (well)/GaAs CB (barrier) SL potential [Fig. 2(b)]. The resulting energy dispersion relation of the SL is schematically shown in Fig. 2(d). What is to be noted here is the PR signal intensity. The signal intensity of the  $E_+$  band transitions of conventional GaAsN alloys in modulation spectroscopies is typically 1/10 or less compared with that of the  $E_-$  band transition.<sup>4–7)</sup> On the other hand, as shown in Fig. 1, the  $E_+$  miniband transitions in the N  $\delta$ -doped SL are comparable in intensity to that of the  $E_-$  miniband transition. This result indicates the formation of distinct  $E_+$  related bands and a fine intermediate energy band structure.

To estimate how much conversion efficiency can be expected in solar cells using a GaAs:N  $\delta$ -doped SL as an absorber, we analyzed theoretically the performance of IBSCs. We have indicated that the miniband energies in GaAs:N  $\delta$ -doped SLs are well described by the Krönig–Penny model if N  $\delta$ -doped layers are treated as equivalent to thin GaAsN alloy layers in which the band edge energies of the  $E_+$  and  $E_-$  bands are determined by the band anti-crossing (BAC) model<sup>4)</sup> and the effective width of the thin GaAsN layer is assumed to be approximately 1.5 nm.<sup>14)</sup> In the description, the VB modification by N incorporation is not taken into account because the VB offset at GaAsN/GaAs interfaces is much smaller than the CB offset.<sup>17,18)</sup> Controversy still remains about the electron effective mass in GaAsN. Here, the electron effective masses in both the  $E_+$  and  $E_-$  bands are treated as equivalent to that in the GaAs CB. On the basis of the above premises, the energy positions of the minibands in the SLs are estimated for various values of structural parameters such as the SL period and the N area density in a  $\delta$ -doped layer. Then, the conversion efficiency under the black-body radiation at 5760 K is calculated by the detailed balance model<sup>19)</sup> in which

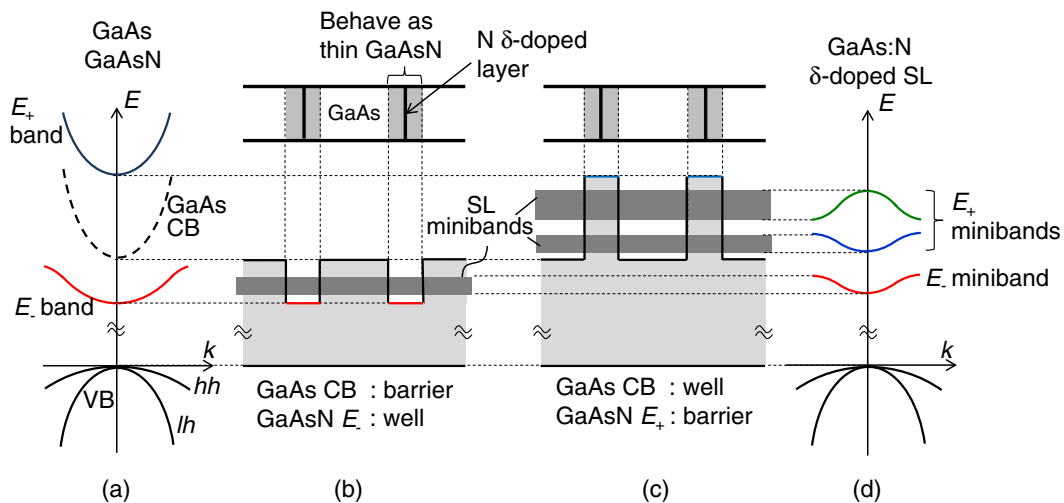


**Fig. 2.** (Color online) Schematic illustration of the energy structure of a GaAs:N  $\delta$ -doped SL. The  $E_+$  and  $E_-$  bands are formed around the  $\delta$ -doped layers. These regions are treated as thin GaAs layers with an effective width. (a) Energy dispersion relations of GaAs and GaAsN (superposed). (b) SL potential consisting of GaAsN  $E_-$  band (well) and GaAs CB (barrier). (c) SL potential consisting of GaAsN  $E_+$  band (barrier) and GaAs CB (well). (d) Energy dispersion relation of the GaAs:N  $\delta$ -doped SL.

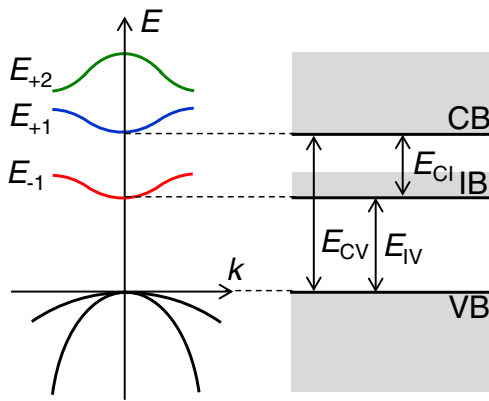


**Fig. 3.** (Color online) Energy dispersion relation of a GaAs:N  $\delta$ -doped SL (left) and the intermediate band structure taken into account in the analyses (right) which consist of the VB, the first miniband of the  $E_{-}$ -related SL potential (labeled  $E_{-1}$ ) and the first miniband of the  $E_{+}$ -related SL potential (labeled  $E_{+1}$ ).

intermediate band structures consist of the VB, the first miniband of the  $E_{-}$ -related SL potential (labeled  $E_{-1}$ ), and the first miniband of the  $E_{+}$ -related SL potential (labeled  $E_{+1}$ ) (see Fig. 3). The results are shown in Fig. 4. Figure 4(a) shows the average N content in GaAs:N  $\delta$ -doped SLs as functions of the SL period and the N area density in a  $\delta$ -doped layer. Figures 4(b) and 4(c) are the mappings of  $E_{CV}$  and  $E_{IV}$ , respectively, in the same range as in Fig. 4(a).  $E_{CV}$  is the energy difference between the  $E_{+1}$  miniband bottom and the VB top, whereas  $E_{IV}$  is that between the  $E_{-1}$  miniband bottom and the VB top. As can be seen in the figures, the larger N content in the SL leads to a larger  $E_{CV}$  and a smaller  $E_{IV}$ . In addition,  $E_{CV}$  is relatively more sensitive to the SL period rather than to the N area density, while  $E_{IV}$  has the opposite tendency. The conversion efficiency is determined by the combination of the values of  $E_{CV}$  and  $E_{IV}$ . Figures 4(d) and 4(e) are the conversion efficiency mappings of IBSCs with GaAs:N  $\delta$ -doped SLs under 1 sun and full concentrated illumination (corresponds to 46200 suns), respectively. By properly adjusting the structural parameters of the SL, high efficiencies of 42.4% for 1 sun and 62.6% for full concentration can be expected. The value of 62.6% is close to the maximum efficiency of IBSCs,<sup>19)</sup> meaning a high potential of this material system as a solar cell absorber. The areas of the optimum efficiency are roughly in agreement between the 1 sun and full concentrated conditions. From a comparison of Figs. 4(d) and 4(e) with Fig. 4(a), it is suggested that the optimum value of the average N content in the SL is within the range from 3 to 4%. N-containing GaAs alloys with this range of N content can be obtained, as has been demonstrated by conventional growth methods such as molecular beam epitaxy<sup>20)</sup> and MOVPE.<sup>21)</sup> In addition, N  $\delta$ -doping into a GaAs layer with the N coverage of up to 0.5 ML (corresponding to the area density of  $3.1 \times 10^{14} \text{ cm}^{-2}$ ), which covers the optimum efficiency in the maps in Figs. 4(d) and 4(e), has been also demonstrated.<sup>11)</sup> However, a certain thickness of the SL layer is required as a solar cell absorber to sufficiently absorb incident light. The strain in the SL layers grown on GaAs substrates may cause a decrease in the critical thickness and poor crystalline quality. Alloying In to the GaAs:N system increases the lattice constant, and thus a lattice mismatch

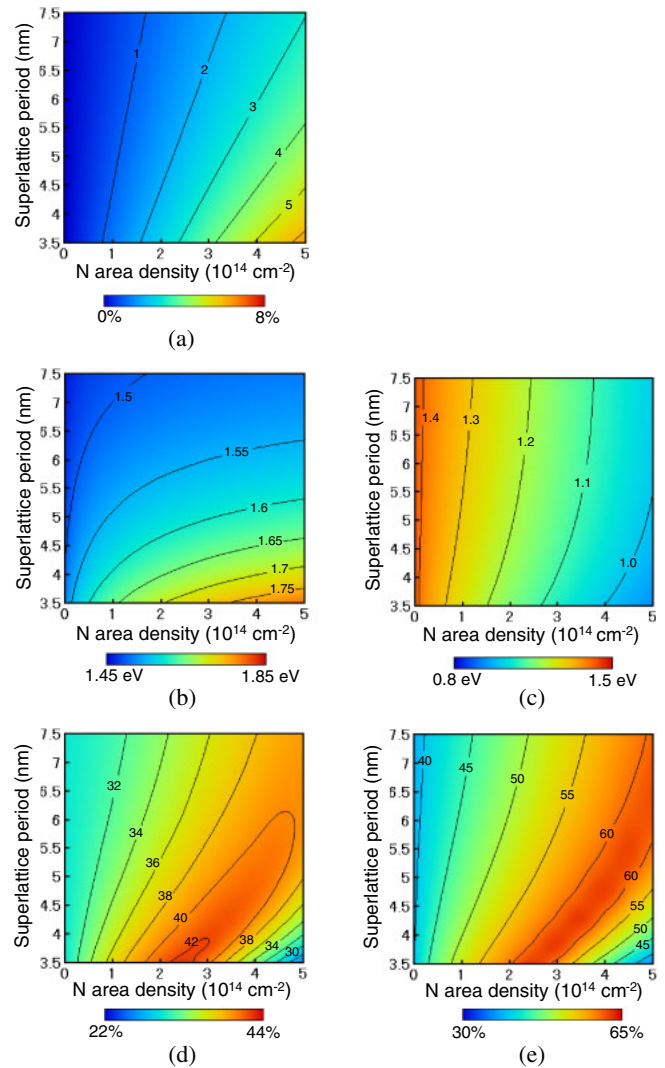


**Fig. 4.** (Color online) Mappings of the (a) average N content in GaAs:N  $\delta$ -doped SLs, (b)  $E_{CV}$ , and (c)  $E_{IV}$ . (d, e) Conversion efficiency of IBSCs with GaAs:N  $\delta$ -doped SLs under (d) 1 sun and (e) full concentrated illumination (46200 suns), respectively. These are shown as functions of the SL period and the N area density in a  $\delta$ -doped layer.

with GaAs substrates can be avoided by using InGaAs instead of GaAs as a host material of N  $\delta$ -doped SLs if the In mole fraction is approximately three times the average N mole fraction in the SLs. As an example, the conversion efficiency of IBSCs based on InGaAs:N  $\delta$ -doped SLs with the SL period of 6 nm is calculated as a function of the N area density in a  $\delta$ -doped layer. The results are shown in Fig. 5. Here, the In content in the InGaAs host matrix is adjusted in such a way that the lattice matching with GaAs is maintained. Parameters in the calculation other than the bandgap and effective mass of the host material are the same as those in the case of GaAs:N  $\delta$ -doped SLs. As can be seen in the figure, the equivalent optimum efficiency can be expected for the In-containing SLs with lower N area density compared with GaAs:N  $\delta$ -doped SLs. The formation of the  $E_{+}$  band and intermediate band energy structures has been confirmed in other dilute nitride semiconductors such as AlGaAsN<sup>4)</sup> and GaAsPN.<sup>22)</sup> Therefore, as we have indicated above, alloying other elements to GaAs:N  $\delta$ -doped SLs is suggested to further facilitate the fabrication of intermediate band materials for high-efficiency solar cells.

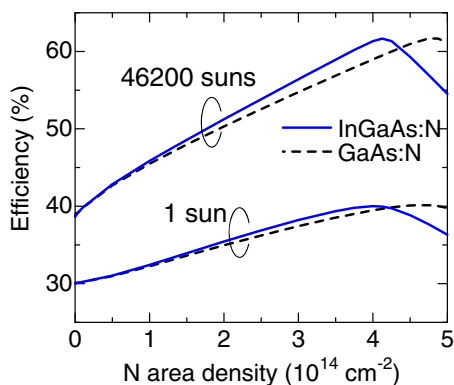


**Fig. 5.** (Color online) Conversion efficiency of IBSCs based on a GaAs:N  $\delta$ -doped SL and an InGaAs:N  $\delta$ -doped SL with the SL period of 6 nm as a function of the N area density in a  $\delta$ -doped layer. The In content in the InGaAs:N  $\delta$ -doped SL is 3 times the average N content.

#### 4. Conclusions

The performance of IBSCs with a GaAs:N  $\delta$ -doped SL as an absorber was analyzed. The conversion efficiency limits were investigated by the detailed balance model based on intermediate band structures composed of the VB and two minibands formed respectively in the  $E_-$ - and  $E_+$ -related SL potentials. It is revealed that high efficiencies of 42.4% for 1 sun and 62.6% for full concentration can be expected by properly adjusting the structural parameters of the SL. In addition, we have shown that alloying other elements such as In to GaAs:N  $\delta$ -doped SLs is a possible way to further facilitate the development of intermediate band materials for high-efficiency solar cells.

- 1) E. Cánovas, A. Marti, A. Luque, and W. Walukiewicz: *Appl. Phys. Lett.* **93** (2008) 174109.
- 2) N. López, L. A. Reichertz, K. M. Yu, K. Campman, and W. Walukiewicz: *Phys. Rev. Lett.* **106** (2011) 028701.
- 3) N. Ahsan, N. Miyashita, M. M. Islam, K. M. Yu, W. Walukiewicz, and Y. Okada: *Appl. Phys. Lett.* **100** (2012) 172111.
- 4) W. Shan, W. Walukiewicz, K. M. Yu, J. W. Ager, III, E. E. Haller, J. F. Geisz, D. J. Friedman, J. M. Olson, S. R. Kurtz, and C. Nauka: *Phys. Rev. B* **62** (2000) 4211.
- 5) M. Geddo, T. Ciabattini, G. Guizzetti, M. Galli, M. Patrini, A. Polimeni, R. Trotta, M. Capizzi, G. Bais, M. Piccin, S. Rubini, F. Martelli, and A. Franciosi: *Appl. Phys. Lett.* **90** (2007) 091907.
- 6) A. Grau, T. Passow, and M. Hetterich: *Appl. Phys. Lett.* **89** (2006) 202105.
- 7) J. D. Perkins, A. Mascarenhas, Y. Zhang, J. F. Geisz, D. J. Friedman, J. M. Olson, and S. R. Kurtz: *Phys. Rev. Lett.* **82** (1999) 3312.
- 8) W. Li, M. Pessa, and J. Likonen: *Appl. Phys. Lett.* **78** (2001) 2864.
- 9) W. Li, M. Pessa, T. Ahlgren, and J. Decker: *Appl. Phys. Lett.* **79** (2001) 1094.
- 10) P. R. C. Kent and A. Zunger: *Phys. Rev. Lett.* **86** (2001) 2613.
- 11) F. Ishikawa, S. Furuse, K. Sumiya, A. Kinoshita, and M. Morifuji: *J. Appl. Phys.* **111** (2012) 053512.
- 12) A. M. Nazmul, T. Amemiya, Y. Shuto, S. Sugahara, and M. Tanaka: *Phys. Rev. Lett.* **95** (2005) 017201.
- 13) S. Noguchi, S. Yagi, Y. Hijikata, K. Onabe, S. Kuboya, and H. Yaguchi: *Proc. 38th IEEE Photovoltaic Specialist Conf., 2012*, p. 83.
- 14) S. Noguchi, S. Yagi, D. Sato, Y. Hijikata, K. Onabe, S. Kuboya, and H. Yaguchi: to be published in *IEEE J. Photovoltaics*.
- 15) D. E. Aspnes: *Surf. Sci.* **37** (1973) 418.
- 16) D. E. Aspnes and A. A. Studna: *Phys. Rev. B* **7** (1973) 4605.
- 17) M. Kozhevnikov, V. Narayanamurti, C. V. Reddy, H. P. Xin, C. W. Tu, A. Mascarenhas, and Y. Zhang: *Phys. Rev. B* **61** (2000) R7861.
- 18) T. Kitatani, M. Kondow, T. Kikawa, Y. Yazawa, M. Okai, and K. Uomi: *Jpn. J. Appl. Phys.* **38** (1999) 5003.
- 19) A. Luque and A. Marti: *Phys. Rev. Lett.* **78** (1997) 5014.
- 20) K. Uesugi, I. Suemune, T. Hasegawa, T. Akutagawa, and T. Nakamura: *Appl. Phys. Lett.* **76** (2000) 1285.
- 21) F. Nakajima, S. Sanorpim, W. Ono, R. Katayama, and K. Onabe: *Phys. Status Solidi A* **203** (2006) 1641.
- 22) K. M. Yu, W. Walukiewicz, J. W. Ager, D. Bour, R. Farshchi, O. D. Dubon, S. X. Li, I. D. Sharp, and E. E. Haller: *Appl. Phys. Lett.* **88** (2006) 092110.